

# Do Molecules as Small as Neopentane Induce a Hydrophobic Response Similar to That of Large Hydrophobic Surfaces?

X. Huang, C. J. Margulis,<sup>†</sup> and B. J. Berne\*

Department of Chemistry and Center for Biomolecular Simulation, Columbia University, 3000 Broadway, New York, New York 10027

Received: May 23, 2003; In Final Form: July 29, 2003

This is the first of two papers aimed at understanding, from an atomistic perspective, hydrophobicity at different length scales and how properties such as local densities and angular profiles change for hydrophobic solutes of different sizes. In a subsequent publication we will describe the hydrophobic hydration and hydrophobic interaction of platelike molecules of nanoscale size. Molecular dynamics is used to compute radial and orientational distribution functions of water around three different molecules: argon, methane, and neopentane. In addition, the potential of mean force between two neopentane molecules is computed. The results for the full OPLS/AA<sup>1</sup> force field are compared with the solute–solvent WCA truncated OPLS/AA force field for these systems. This work addresses the question of whether a molecule of the size of neopentane is large enough to induce a hydrophobic response similar to that of large hydrophobic molecules or paraffin walls. We answer this question in the affirmative. The orientational distribution of water molecules in the first shell neighboring the neopentane molecule is very similar to that near a paraffin wall, in contrast to argon and methane. In addition, the potential of mean force between two neopentane molecules, with the WCA truncated OPLS/AA potential, displays a dewetting-like transition much like that found between two macroscopic hydrophobic objects. We conclude that neopentane defines a length scale for the observation of large-scale hydrophobicity. Smaller molecules fit into a water clathrate, whereas larger molecules force the water to reorganize such that there are dangling OH bonds pointing toward the hydrophobic surface. Large-scale hydrophobicity arises in solute molecules as small as neopentane with diameter ( $d \approx 5.2$  Å).

## 1. Introduction

The introduction of a sufficiently large solute molecule into a bulk liquid can induce a depletion of solvent next to the solute molecule.<sup>2–9</sup> This depletion is sensitive to the strength of the attractive forces between the solute and solvent and to the interfacial properties of the solvent.<sup>3</sup> For solvents with high liquid–vapor surface tensions such as water, solvent depletion is less favorable than for solvents with low surface tension. Put another way, for solvent depletion to occur, a solute molecule in water must be larger than in lower surface tension solvents. Dewetting has been observed in simulations in explicit water between two nanometer-sized oblate ellipsoidal plates,<sup>6,7</sup> in transition path sampling studies of confined Lennard-Jones systems,<sup>10</sup> and in the study of drying using coarse-grained treatments of liquid water.<sup>11–15</sup> A successful theory of this drying phenomenon has been presented by Lum, Chandler, and Weeks (LCW).<sup>2,3</sup> This theory spans both small and large length scales, predicting drying only for sufficiently large length scale solutes. The nanometer length scale on which drying has been observed to occur has caused investigators to wonder whether this phenomenon is relevant to the thermodynamics and kinetics of protein folding<sup>16</sup> where, it is believed, the initial stages of folding is caused by the collapse and aggregation of strongly hydrophobic amino acid residues. It is of some importance, therefore, to determine the smallest length scale on which this

depletion and reorganization of water will occur and to understand how attractive solute–solvent forces influence these phenomena.

In this paper we address small length scale hydrophobicity. In a subsequent paper<sup>41</sup> we address the large-scale hydrophobicity. This paper is in a sense an extension of earlier papers on hydrophobic hydration and the hydrophobic interaction of noble gas atoms in water.<sup>17,18</sup> In those papers computer simulations were used to determine how water organizes around noble gas atoms and around pairs of noble gas atoms as a function of the relative distance from each other. It was found that atoms fit into small clathrate cages without diminishing the number of hydrogen bonds per water molecule.<sup>4,16,17–19</sup> The potential of mean force (PMF) between noble gas atoms was determined as a function of relative distance, and it was found that this had two minima: a solvent-separated minimum and a contact minimum. The solvent separated minimum was found to be more probable than the contact minimum. Thus, for small hydrophobic solutes it was found that the hydrophobic effect was much smaller than expected at that time. Two small solutes can fit into the network of hydrogen bonds without distorting it much. This is in marked contrast to what is expected for large solutes. For sufficiently large solutes the hydrogen bond network will become distorted,<sup>2,8</sup> and as we show in this paper, some of these bonds will be destroyed, leading to dangling hydrogen bonds. For what solute particle size will this happen? In surface tension terms, the surface tension of a surface with dangling hydrogen bonds will be different than for a surface with intact hydrogen bonds.

<sup>†</sup> Current address: Department of Chemistry, University of Iowa, 319 CB, Iowa City, Iowa 52242.

There have been several experimental<sup>20–22</sup> and theoretical papers<sup>3,8,23,24</sup> analyzing the structural features of water molecules in contact with large paraffin-like surfaces, biological molecules, and liquid–vapor interfaces. It is well established from computer simulations that a hydrophobic surface differs considerably from what is found near small hydrophobic solute molecules in bulk solution.<sup>3,6,7,25</sup> Second harmonic generation experiments show that water molecules adjacent to a liquid–vapor interface display a very distinct equilibrium angular distribution which is different from that in the bulk.<sup>20–22</sup> It is thus important to understand hydrophobicity on small and large length scales. In the present paper we pose two well-defined questions: Do water molecules solvating medium size organic solutes display any of the characteristics known from simulations to be present at a large hydrophobic interface? How do solvent–solute attractions influence the hydrophobic phenomena in the small to medium size organic molecule regime? We try to establish how large an organic molecule must be in order for its proximate water molecules to display the characteristic features of larger hydrophobic surfaces.

To address these questions, we study two signatures of a hydrophobic interface. It has been shown computationally that water molecules adjacent to a hydrophobic surface display angular distributions such that a dangling O–H group points into the hydrophobic phase.<sup>8</sup> The distribution function of the angle between the water dipole vector and the unit vector that points from the oxygen atom normal to the hydrophobic surface will be one of the signatures that we will monitor in our simulations. The other important variable that we monitor is the water density profile around a particular solute. Explicit simulations of large hydrophobic surfaces have been carried out in the past by Berne and co-workers,<sup>6</sup> by Chandler et al.,<sup>10</sup> by Rossky et al.,<sup>8</sup> and by others.<sup>13,26</sup> It is important to note that some of these early studies were done under constant volume conditions so that drying or dewetting cannot occur; nevertheless, the liquid found in between these surfaces presents a characteristic density profile which we use as a benchmark to compare against our simulations of small molecules dissolved in water.

We know that hydrophobic hydration and hydrophobic interaction are related phenomena, but we do not know whether these two begin to occur exactly at the same length scale. Being more specific, will a pair of solvent molecules large enough to present angular distributions similar to those observed when water is adjacent to a large hydrophobic surface also expel the solvent when brought close together? Will the attractive part of the potential between the solvent and solute play any role at all in these results?

To analyze the differences and similarities between what is observed at large hydrophobic interfaces and at small organic solute systems, we performed two different studies. The first one aimed at understanding the properties of single solute molecules. In this study of hydrophobic hydration we monitor the water density profile around a single hydrophobe as well as the angular distribution of the dipole vectors of the different water molecules with respect to a unit vector that points from the oxygen atom of each water molecule toward the center of the solute as shown in Figure 1.

In the second part of this paper we focus on the phenomenon of drying and collapse due to the hydrophobic interaction. Here we compute potentials of mean force between solute molecules. We remove the direct contribution of the solute–solute potential from the potential of mean force and thereby obtain the solvent-induced contribution which is the driving free energy responsible

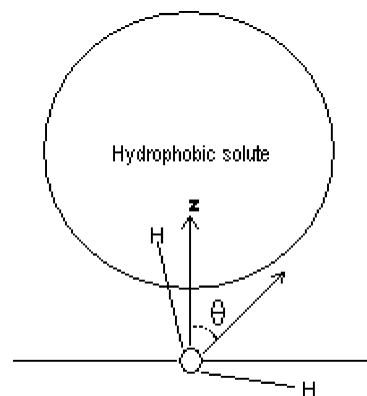


**Figure 1.** Definition of  $\cos(\theta)$  the angle between a water molecule's dipole vector and the unit vector pointing from the oxygen atom in water toward the center of a hydrophobic solute.

for hydrophobic interaction. We performed this analysis for both the full OPLS/AA potential and for the WCA truncated interaction potential between solute and solvent molecules. From this we gain an understanding of the role that weak attractions play in the phenomenon of hydrophobic-induced drying and collapse and thus are able to predict that organic molecules of the size of neopentane display a borderline character between the small and large length-scale regime.

## 2. Methods

We performed classical molecular dynamics simulations to investigate the water structure around solute molecules of different sizes (argon, methane, and neopentane). The simulated systems consisted of a single solute molecule or atom in explicit water. The SPC model<sup>27</sup> of water is used in this work. The parameters for argon, methane, and neopentane were taken from the OPLS/AA force field.<sup>1</sup>

To separate the effect of the attractive part of the potential in each of these systems, we performed two different simulations: the first one using the full OPLS/AA force field and the second one using the WCA truncated repulsive solute–solvent interaction.<sup>28</sup> Molecular dynamics was employed using the RATTLE<sup>29</sup> procedure to constrain the internal geometry of the SPC water molecules. Periodic boundary conditions were implemented, and the particle–particle particle–mesh Ewald method<sup>30,31</sup> was employed to treat long-range electrostatic interactions. The reference system propagator algorithm (r-RESPA)<sup>30,32,33</sup> was employed with a time step of 0.5 fs for the fast, short-range intramolecular forces and 2 fs for the slower degrees of freedom. All simulations were performed at constant temperature (298.15 K) and pressure (1 atm) with Nose–Hoover chain (NHC) thermostats and an Andersen–Hoover-type barostat<sup>34,35</sup> using the program SIM developed in our group.<sup>36</sup>

For the hydrophobic hydration study, a simulation box with 343 water molecules was first equilibrated for 150 ps, then the solute molecule was introduced in the simulation box, and the overlapping water molecules were removed. The new system was equilibrated for another 50 ps. The production runs were 1.4 ns long in duration.

To study the hydrophobic interaction, the simulated system consisted of two solute molecules in explicit water. The potential of mean force for different solute pairs was computed using the umbrella sampling procedure. A quadratic restraining potential was used to bias the distance between the centers of mass of the solute molecules, but the effect of this bias was

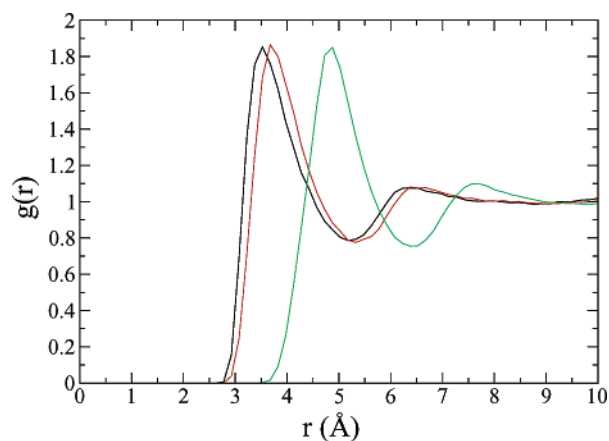


**Figure 2.** Comparison of water radial distribution functions around argon (black), methane (red), and neopentane (green) using the full OPLS/AA interaction potential.

then removed. Data for 15 different windows corresponding to distances between  $r_0 = 4$  Å and  $r_0 = 18$  Å were collected. The force constant used for the biasing potential was 2 kcal/(mol Å<sup>2</sup>).

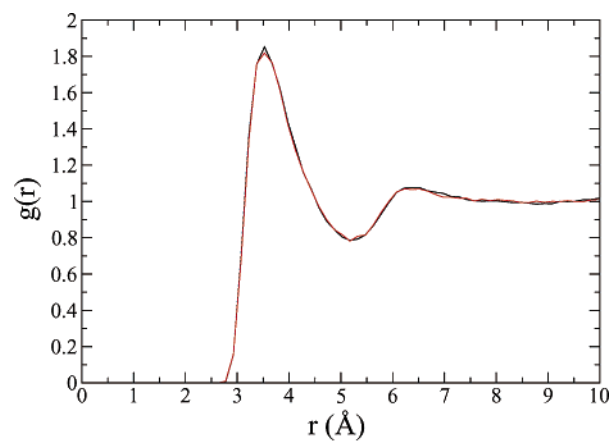
The simulation box which initially consisted of 2048 water molecules was first equilibrated for 150 ps, then the solute molecules were introduced, and overlapping solvent molecules were removed. For each window, the system was equilibrated for 20 ps, and data was collected on subsequent 400 ps runs. Potentials of mean force were computed from the biased distributions using the same procedure as in Pangali et al. and references therein.<sup>17,18</sup>

### 3. Results

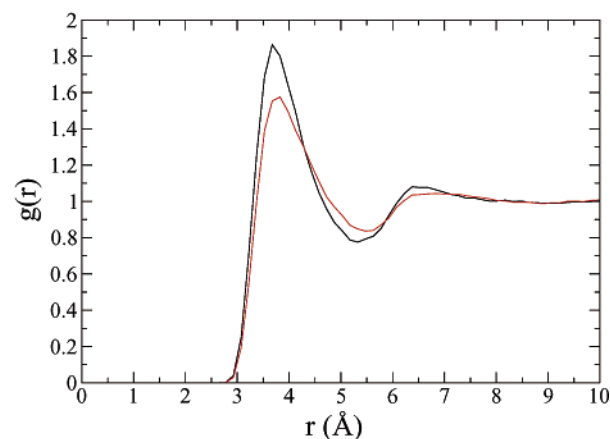
**3.1. Hydrophobic Hydration.** Radial distribution functions displayed in Figure 2 were computed between water oxygen atoms and the center of mass in the argon, methane, and neopentane systems. By comparing these three distribution functions, it is clear that, apart from a shift at the origin which is due to the different hard-core diameters, they are for all purposes identical. The question arises as to whether the attractive part of the interaction potential between water and the solute atom or molecule plays a significant role in hydrophobic hydration. Clearly argon, methane, and neopentane have different strength attractive interactions with water. This however does not seem to affect the structure of the solute–solvent radial distribution functions for these different solutes.

Parts a, b, and c of Figure 3 display a comparison of the density profiles for liquid water around argon, methane, and neopentane, respectively, obtained from our MD simulations using the full OPLS/AA and WCA truncated potentials between the solute and solvent. It is clear from these figures and from Figure 2 that for the full solute–solvent OPLS/AA potentials the shapes of the solute–solvent pair correlation function,  $g(r)$ 's, are almost identical, with the position of the first peak scaling with molecular size. Yet for the WCA truncated potentials, the shape of the  $g(r)$ 's changes dramatically with solute size. This effect of solute size occurs only when the attractions are removed, that is, when the truncated WCA potential is used.

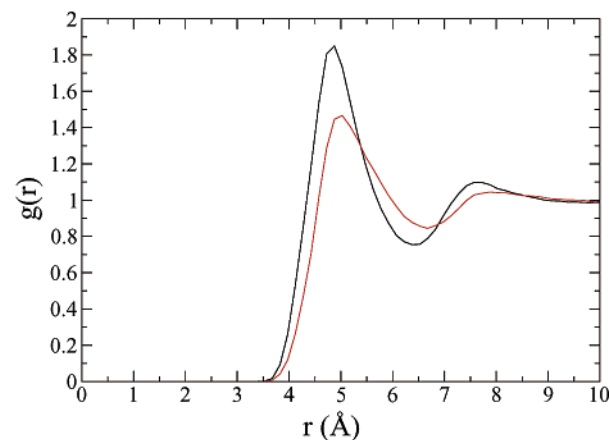
It is obvious from Figure 3a that the local water density around an argon molecule does not change appreciably when attractive interactions are turned off. From this we draw two conclusions: (1) For small molecules like argon (basically the same size as water), typical attractive interactions do not change the density profile from what is observed for the WCA truncated



(a)



(b)



(c)

**Figure 3.** (a), (b), and (c) display radial distribution functions for water around argon, methane, and neopentane using the full OPLS/AA potential (black) and WCA type interactions (red) between solute and solvent molecules.

potential. (2) For small molecules like argon, the first peak of  $g(r)$  is higher than that expected when water is close to a hydrophobic interface.

In Figure 3b, we see that for methane the two distribution functions are similar; however, the first peak of  $g(r)$  in the case of the full potential calculation is higher and narrower than for the truncated WCA potential, that is, when attractions are removed. Figure 3c corresponds to the neopentane case; here

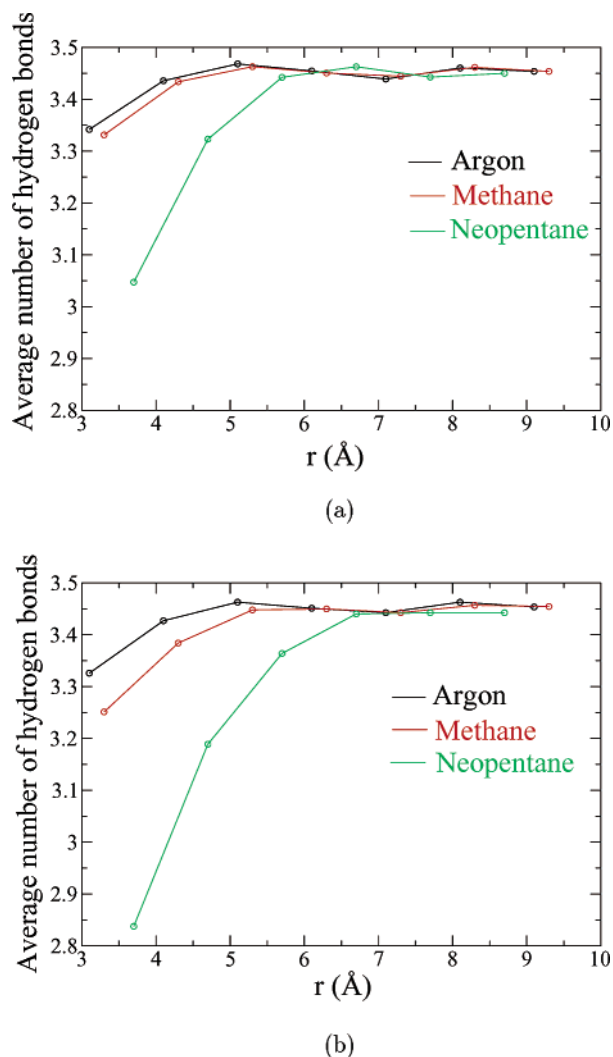


**Figure 4.** (a) and (b) display the average number of hydrogen bonds in spherical shells of 1 Å around argon, methane, and neopentane in the case of the full potential (a) and WCA (b) type interactions.

we note that the two distribution functions are significantly different. Although the height of the first peak for the full potential is still about 1.9, the height for the truncated WCA case is only 1.45. This density profile is remarkably similar to that obtained by Berne and co-workers<sup>6,7</sup> when analyzing the density distribution of water around one large hydrophobic plate. It should also be noted that in the WCA truncated simulation the position of the first peak is shifted away from the solute by about 0.3 Å compared to that of the full potential. The attractive part of the potential effectively makes the first shell move closer to the solute. Here we conclude that the density profile around WCA truncated neopentane is very similar to that found around very large hydrophobic surfaces. A previous study using LCW theory<sup>3</sup> predicts a similar behavior of the water radial distribution functions around hydrophobic solutes.

Parts a and b of Figure 4 display the average number of hydrogen bonds per water molecule in spherical shells around argon, methane, and neopentane for the full potential and WCA type interactions, respectively. A water pair is hydrogen bonded if<sup>37,38</sup> the oxygen–oxygen distance,  $R_{OO}$ , is no greater than 3.5 Å and simultaneously the bonded H–O···O angle,  $\alpha$ , is no greater than 30°. There is a clear qualitative difference between what is observed in the case of neopentane and the other solutes. The hydrogen bond network must be broken to accommodate a neopentane molecule, but no significant loss of hydrogen

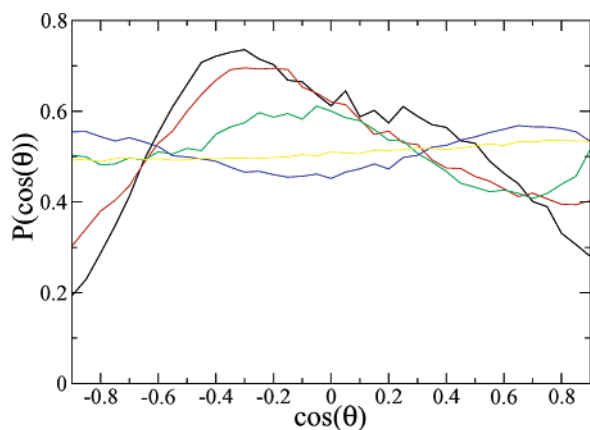
bonds is observed for smaller size solutes. Thus, we conjecture that neopentane represents a crossover size between small and large solute hydrophobicity. For solute particles larger than neopentane, water behaves much like it does around large hydrophobic interfaces.

**3.2. Orientational Distributions.** Bulk water is homogeneous and isotropic, but the presence of a liquid–vapor or a liquid–solid interface breaks this symmetry. It is of considerable interest to explore the orientations of water molecules with respect to their distance from the interface. Here we focus on the orientation of the water dipole vector,  $\hat{\mu}$ , with respect to the outward normal  $\hat{u}$  to the interface pointing from liquid to vapor (or solid, or solute), as shown in Figure 1. We study the distribution function of  $\cos \theta \equiv \hat{\mu} \cdot \hat{u}$  in successive layers of thickness  $\Delta z = 1.0$  Å from the interfacial layer down to layers far from the interface (in the bulk). Lee et al.<sup>8</sup> determined this  $\cos \theta$  for the water–paraffin interface (in the  $\{N, V, T\}$  ensemble), and Garrett et al.<sup>23</sup> computed this quantity for the water–vapor interface. Next to the interface (or hydrophobic wall), the distribution function,  $P(\cos \theta)$ , was found to display a pronounced maximum at a positive value of  $\cos \theta$ , but in the next layer down, the maximum in  $P(\cos \theta)$  shifts to a negative value of  $\cos \theta$ . For subsequent layers down, the maximum shifts from negative values of  $\cos \theta$  toward  $\cos \theta \approx 0$  and becomes flatter until one gets deep enough into the liquid where the maximum disappears altogether, and the orientational distribution becomes isotropic—as one expects for the bulk phase.

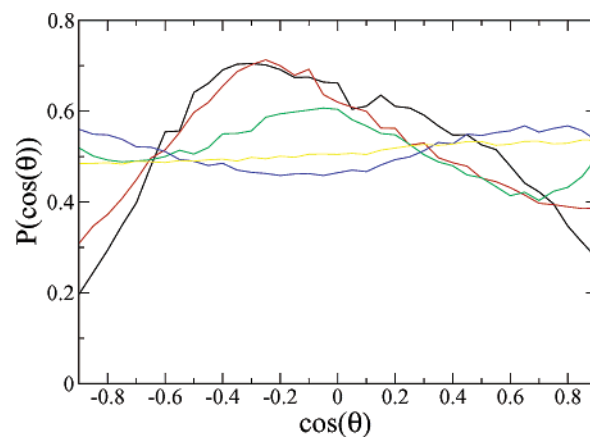
Given the observed orientational distribution behavior near a macroscopic hydrophobic interface, it is interesting to ask whether this orientational behavior will persist in the neighborhood of a small- or intermediate-sized hydrophobic solute molecule. How large must this hydrophobic solute molecule be for the neighboring water molecules to display the characteristic shift in the orientational distribution between the first layer and the next? Do attractive interactions between this solute molecule and water molecules affect the orientational distribution?

To answer these questions, we carried out computer simulations on a set of molecules of increasing size, namely, argon ( $\sigma = 3.4$  Å), methane ( $\sigma = 3.6$  Å), and neopentane ( $\sigma = 5.2$  Å). We determined the distribution functions,  $P(\cos \theta)$ , of the water molecules in spherical shells around the center of mass of each solute molecule. The width of these shells was taken to be 1 Å. These orientational distributions are shown for the full OPLS/AA potentials in Figure 5. We note that for neopentane the mean value of  $\cos \theta$  in the first shell has an opposite sign to that in all subsequent ones. As one moves further away from the solute molecule, these distribution functions become flatter, reaching the limit of a uniform distribution as expected from dipoles that orient randomly. This is exactly the same behavior observed next to a macroscopic hydrophobic object. The angular distribution we computed for water around neopentane is strikingly similar to that found in the simulations of infinite hydrophobic walls of Rossky<sup>8</sup> and the simulations of liquid/vapor interface of Garret et al.<sup>20,21</sup> The most probable orientation in the first shell is that with one hydrogen-bonding group aligned so as to point toward the hydrophobic surface. The mean angle in the next two contiguous shells has the O–H direction tangential to the surface. No preferred orientation is found for water molecules in the bulk portion of the simulation cell. In the case of argon and methane the characteristic shift in the distribution function between the first and subsequent shells is absent and therefore does not resemble what is observed at large hydrophobic interfaces.

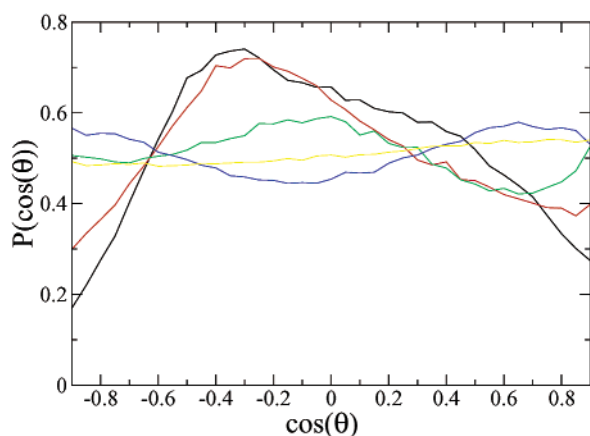




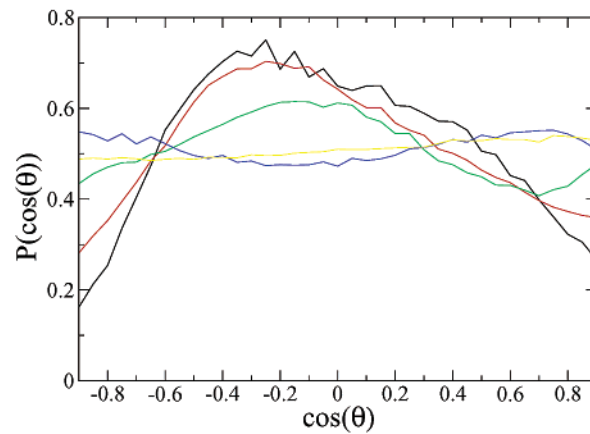
(a)



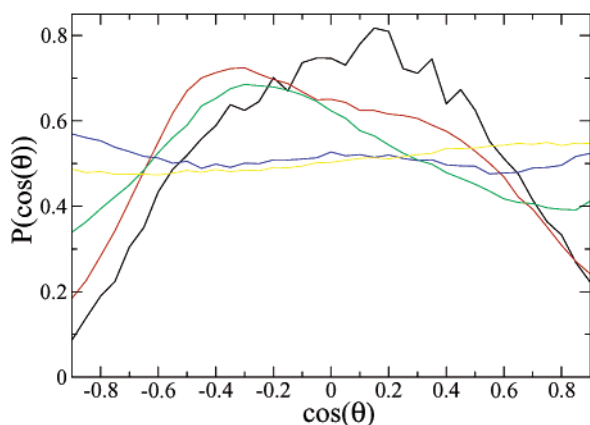
(a)



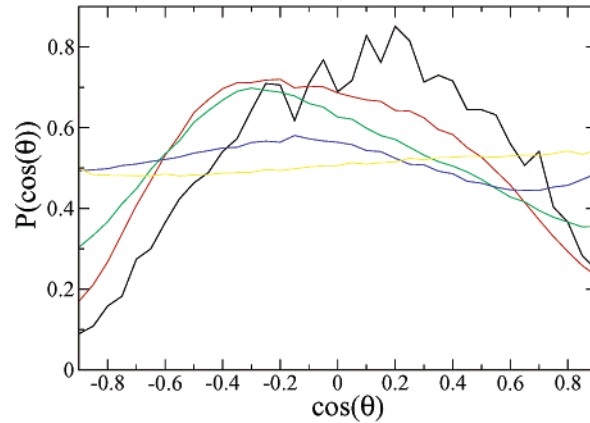
(b)



(b)



(c)



(c)

**Figure 5.** (a), (b), and (c) display angular distribution between vectors defined in Figure 1 for argon, methane, and neopentane, respectively, using the full OPLS/AA type interaction between solute and solvent. Argon: black, red, green, blue, and yellow correspond to 2.6–3.6, 3.6–4.6, 4.6–5.6, 5.6–6.6, and 10–11 Å, respectively. Methane: black, red, green, blue, and yellow correspond to 2.8–3.8, 3.8–4.8, 4.8–5.8, 5.8–6.8, and 10–11 Å, respectively. Neopentane: black, red, green, blue, and yellow correspond to 3.2–4.2, 4.2–5.2, 5.2–6.2, 6.2–7.2, and 10–11 Å, respectively.

To determine whether the attractive part of the solute–solvent potential plays an important role in determining the orientational distribution, we simulated the system with WCA truncated solute–solvent potentials. As can be observed from Figure 6,

**Figure 6.** (a), (b), and (c) display angular distribution between vectors defined in Figure 1 for argon, methane, and neopentane, respectively, using the WCA-type interaction between solute and solvent. Color code is the same as in Figure 5.

these distributions follow the same trend observed for the full OPLS/AA interaction. WCA argon and methane do not show the signature of a macroscopic interface while WCA neopentane does.

**3.3. Hydrophobic Interaction.** In this section, we focus on the hydrophobic interaction between two solute molecules. Since the orientational distribution of water molecules around a single neopentane molecule, but not around the smaller solutes argon

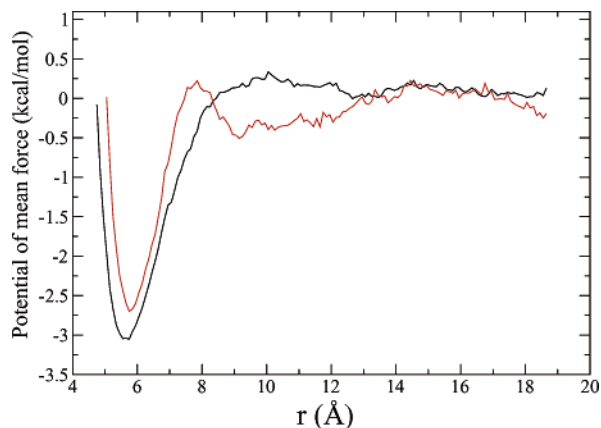


**Figure 7.** Comparison between the potential of mean force obtained for a pair of neopentane molecules in SPC water when solute-solvent attractions are included (red) and in the case of WCA type interaction (black).

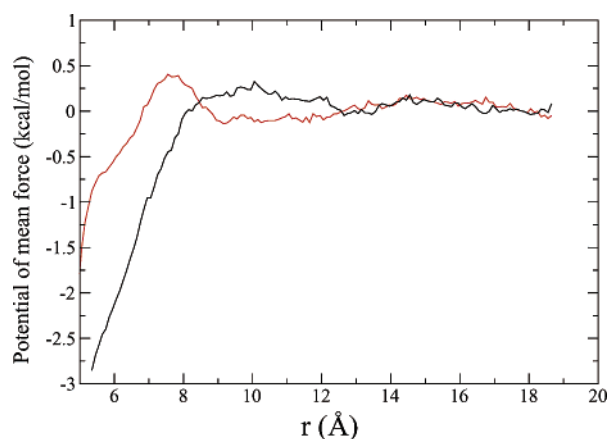


**Figure 8.** Solvent contribution to the potential of mean force obtained for a pair of neopentane molecules in SPC water when solute-solvent attractions are included (red) and in the case of WCA type interaction (black).

and methane, shows the signature found for macroscopic hydrophobic surfaces, will two neopentane molecules at close separation display the kind of drying we have seen when two large hydrophobic plates are brought closer than a critical distance?<sup>6</sup> Does neopentane display interesting borderline behavior intermediate between large hydrophobic surfaces and small molecules?

By following the procedure described in the method section, we obtained the neopentane-neopentane potential of mean force  $W(r)$  in water as a function of distance between the center of mass of each molecule. This was done both for the WCA truncated and full potential type interactions between solute and solvent molecules. Results are displayed in Figure 7. We also isolated the solvent contribution to the potential of mean force,  $\Delta W(r)$ , by subtracting the direct solute-solute potential function,  $V(r)$ , from the potential of mean force,  $W(r)$ ; a comparison between  $\Delta W(r)$  for the full and the WCA truncated potentials is displayed in Figure 8.

The results we obtain for the potential of mean force are consistent with previous calculations by Garde and co-workers<sup>39</sup> using a different force field. For the full potential one finds two minima: one with the two molecules in contact and hence no water molecules in between and the other minimum corresponding to two neopentanes separated by one water layer. The free energy difference between the solvent-separated minimum and the contact minimum is approximately 2.25 kcal/

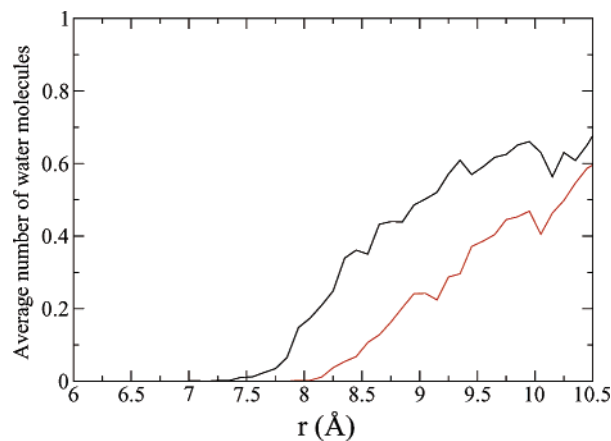


**Figure 9.** Average number of water molecules found in the region between neopentane molecules as a function of their interparticle distance  $r$ . The region is defined to be a cylinder of diameter  $d = 2.8$  Å whose base intersects each of the neopentane molecules. The black line is for the full OPLS/AA potential, and the red line is for the WCA truncated case.

mol. The free energy barrier to go from the pair in contact to the solvent-separated pair is approximately 3.0 kcal/mol, and for the reverse process it is 0.75 kcal/mol. The situation for the WCA truncated potential is qualitatively different. Here the PMF  $W(r)$  does not exhibit any well-defined solvent separated minimum; that is, there is no stable configuration with one water layer between the two neopentanes at short distances. The solvent-separated minimum present in the case of the full OPLS/AA potential PMF has totally disappeared. The probability distribution of a given separation  $r$ ,  $\approx 4\pi r^2 \exp(-\beta W(r))$ , is much larger for contact pairing than for solvent-separated pairing for both the full and WCA truncated potentials. This is in contrast to what is observed in the “small molecule regime” where contact pairing is found to be less probable than solvent-separated pairing.<sup>17,18,40</sup>

It is of interest to see whether there is a dewetting phenomenon in neopentane similar to that observed for large hydrophobic plates. To probe this, we determine the number of water molecules found in the region between the two neopentane molecules as a function of their interparticle distance  $r$ . This is shown in Figure 9. From Figure 3 we see that in the liquid the contact distance between a neopentane molecule and water is  $\approx 3.6$  Å; therefore, we would expect that water molecules would be able to fit in between two neopentane molecules when the interparticle distance is 7.2 Å. This appears to be the case for the full OPLS/AA type of interaction, but not for the WCA truncated potential. We thus conclude that if the contact pair is separated to a distance where one water molecule should be able to fit in between the pair, no water molecule is found there in the case of the WCA truncated potential. This depletion of water density between two neopentane molecules is similar to what Berne and co-workers<sup>6</sup> observed in the past for the case of two large ellipsoids. Neopentane is the smallest molecule so far that exhibits “large molecule” dewetting behavior and thus represents the dividing point between small and large molecule behavior.

#### 4. Conclusions

In this work we explored how solute size and solute-solvent attractive forces affect hydrophobic hydration and hydrophobic interaction. We find that small organic molecules like neopentane display many of the characteristics that one expects to find only in very large hydrophobic objects. The angular distribution

of water molecules neighboring a neopentane molecule is strikingly similar to that found next to a macroscopic hydrophobic interface. Similarly, the density profile of water between a pair of neopentane molecules exhibits a kind of drying expected between two large hydrophobic surfaces brought close together. In the absence of solute–solvent attractions the similarities between neopentane and large hydrophobic objects become even more pronounced. None of the signatures of the response to large hydrophobic objects are found in the case of argon and methane, not even when the attractive part of the potential is removed.

Why is neopentane different from argon and methane and similar to a macroscopic hydrophobic object? Why do attractions between solvent and solute qualitatively affect the results in the case of neopentane but not in the case of argon? Perhaps the crossover region between typical “small molecule” hydrophobicity and what is observed for macroscopic systems occurs when a solute molecule is much larger than typical cavities generated by normal fluctuations in the solvent density. Hydrogen bonds must be broken to accommodate neopentane molecules and the energy cost paid in this process is larger than available from normal thermal fluctuations. The fact that hydrogen bonds must be broken is clear from the angular distribution of solvent molecules around a single neopentane molecule which shows the same pattern of dangling hydrogen bonds observed in second harmonic generation experiments<sup>21,22</sup> when water is in close contact with a macroscopic liquid–vapor interface. The degree to which hydrophobicity of medium size molecules resembles that of a large hydrophobic object depends on how many hydrogen bonds must be broken to accommodate the solute. Parts a and b of Figure 4 show the average number of hydrogen bonds per water molecule in spherical shells around each of the studied solutes for the case of the full potential and WCA type interaction, respectively. It is clear from these plots that only in the case of neopentane must a significant number of hydrogen bonds be broken for the spherical shell in contact with the solute. This is consistent with our observation that only neopentane displays dangling hydrogen bonds in the water angular distributions. Attractions affect the results in the case of neopentane because they allow water molecules to be 0.3 Å closer than in the case of pure repulsive interactions. This lowers the average number of hydrogen bonds that must be broken because the effective cavity volume in which this molecule exists is smaller. In the case of argon, solvent density profiles, angular profiles, and the distribution of hydrogen bonds around the solute are basically unaffected by the inclusion of attractions between solute and solvent. This is a simple consequence of the fact that no hydrogen bonds must be lost to accommodate a cavity of the size of argon. Obviously argon is a hydrophobic solute, but the nature of hydrophobicity in this case is not energetic but entropic.

The importance of small attractions in the case of neopentane becomes very clear when we observe that the potential of mean force in the presence and absence of these attractions is qualitatively different. In the absence of attractions, when two neopentane molecules are brought together to a distance that should permit one water molecule to be found between them, none is found. This dewetting phenomenon is not found for methane or argon and is typical of larger systems in which drying is observed between hydrophobic objects. We have explored elsewhere these larger nanoscale systems.<sup>41</sup>

**Acknowledgment.** This work was supported by a grant from the National Science Foundation (CHE-00-76279). We have benefited from a generous allocation of computer time from the Boston University Supercomputing Center. We thank Dr. Harry Stern for his help extending “SIM”.

## References and Notes

- (1) Jorgensen, W. L.; Maxwell, D. S.; Tirado-Rives, J. *J. Am. Chem. Soc.* **1996**, *118*, 11225–11236.
- (2) Lum, K.; Chandler, D.; Weeks, J. D. *J. Phys. Chem. B* **1999**, *103*, 4570–4577.
- (3) Huang, D. M.; Chandler, D. *J. Phys. Chem. B* **2002**, *106*, 2047–2053.
- (4) Stillinger, F. H. *J. Solution Chem.* **1973**, *2*, 141–158.
- (5) Hummer, G.; Rasaiah, J. C.; Noworyta, J. P. *Nature (London)* **2001**, *414*, 188–190.
- (6) Wallqvist, A.; Berne, B. J. *J. Phys. Chem.* **1995**, *99*, 2885–2892.
- (7) Wallqvist, A.; Berne, B. J. *J. Phys. Chem.* **1995**, *99*, 2893–2899.
- (8) Lee, C. Y.; McCammon, J. A.; Rossky, P. J. *J. Chem. Phys.* **1984**, *80*, 4448–4454.
- (9) Wallqvist, A.; Gallicchio, E.; Levy, R. M. *J. Phys. Chem. B* **2001**, *105*, 6745–6753.
- (10) Bolhuis, P. G.; Chandler, D. *J. Chem. Phys.* **2000**, *113*, 8154–8160.
- (11) Wolde, P. R. T.; Chandler, D. *Proc. Natl. Acad. Sci. U.S.A.* **2002**, *99*, 6539–6543.
- (12) Lum, K.; Chandler, D. *Int. J. Thermophys.* **1998**, *19*, 845–855.
- (13) Lum, K.; Luzar, A. *Phys. Rev. E* **1997**, *56*, 6283–6286.
- (14) Luzar, A.; Leung, K. *J. Chem. Phys.* **2000**, *113*, 5836–5844.
- (15) Leung, K.; Luzar, A. *J. Chem. Phys.* **2000**, *113*, 5845–5852.
- (16) Chandler, D. *Nature (London)* **2002**, *417*, 491–491.
- (17) Pangali, C.; Rao, M.; Berne, B. J. *J. Chem. Phys.* **1979**, *71*, 2975–2981.
- (18) Pangali, C.; Rao, M.; Berne, B. J. *J. Chem. Phys.* **1979**, *71*, 2982–2990.
- (19) Pratt, L. R.; Chandler, D. *J. Chem. Phys.* **1977**, *67*, 3683–3704.
- (20) Du, Q.; Superfine, R.; Freysz, E.; Shen, Y. R. *Phys. Rev. Lett.* **1993**, *70*, 2313–2316.
- (21) Du, Q.; Freysz, E.; Shen, Y. R. *Science* **1994**, *264*, 826–828.
- (22) Eiselth, K. B. *Acc. Chem. Res.* **1993**, *26*, 636–643.
- (23) Taylor, R. S.; Dang, L. X.; Garret, B. C. *J. Phys. Chem.* **1996**, *100*, 11720–11725.
- (24) Cheng, Y.; Rossky, P. J. *Nature (London)* **1998**, *392*, 696–699.
- (25) Huang, D. M.; Chandler, D. *Phys. Rev. E* **2000**, *61*, 1501–1506.
- (26) Bratko, D.; Curtis, R. A.; Blanch, H. W.; Prausnitz, J. M. *J. Chem. Phys.* **2001**, *115*, 3873–3877.
- (27) Berendsen, H. J. C.; Postma, J. P. M.; van Gunsteren, W. F.; Hermans, J. In *Intermolecular Forces*; Pullman, B., Ed.; Reidel: Dordrecht, Holland, 1981.
- (28) Chandler, D.; Weeks, J. D.; Andersen, H. C. *Science* **1983**, *220*, 787–794.
- (29) Andersen, H. C. *J. Comput. Phys.* **1983**, *52*, 24–34.
- (30) Zhou, R.; Harder, E.; Xu, H.; Berne, B. J. *J. Chem. Phys.* **2001**, *115*, 2348–2358.
- (31) Luty, B. A.; Tironi, I. G.; van Gunsteren, W. F. *J. Chem. Phys.* **1995**, *103*, 3014–3021.
- (32) Tuckerman, M.; Berne, B. J.; Martyna, G. J. *J. Chem. Phys.* **1992**, *97*, 1990–2001.
- (33) Stuart, S. J.; Zhou, R.; Berne, B. J. *J. Chem. Phys.* **1996**, *105*, 1426–1436.
- (34) Martyna, G. J.; Klein, M. L.; Tuckerman, M. E. *J. Chem. Phys.* **1992**, *97*, 2635–2643.
- (35) Martyna, G. J.; Tobias, D. J.; Klein, M. L. *J. Chem. Phys.* **1994**, *101*, 4177–4189.
- (36) Stern, H.; Xu, H.; Harder, E.; Rittner, F.; Pavese, M.; Berne, B. J. SIM molecular dynamics simulation program.
- (37) Luzar, A.; Chandler, D. *Nature (London)* **1996**, *379*, 55–57.
- (38) Starr, F.; Nielsen, J.; Stanley, H. *Phys. Rev. E* **2001**, *62*, 579–587.
- (39) Garde, S.; Hummer, G.; Paulaitis, M. E. *Faraday Discuss.* **1996**, *103*, 125–139.
- (40) Rick, S. W.; Berne, B. J. *J. Phys. Chem. B* **1997**, *101*, 10488–10493.
- (41) Huang, X.; Margulis, C. J.; Berne, B. J. Dewetting-induced collapse of hydrophobic particles. *Proc. Nat. Acad. Sci.* **2003**, in press.